Proceedings of the ICBBG2025
2025 International conference on Bio-mediated and Bio-inspired Geotechnics
18-20 May, 2025 | Tempe, Arizona, USA
https://doi.org/10.53243/ICBBG2025-187

Biochemical Species Plume Migration under Diverse Injection Strategies during Microbially Induced Calcite Precipitation Treatment in Soils

Pavan Kumar Bhukya, S. M. ASCE,[1] Xuerui Wang, Ph.D.,[2] and Dali Naidu Arnepalli, Ph.D., A. M. ASCE[3]

[1]Research scholar, Department of Civil Engineering, Indian Institute of Technology Madras, Chennai, Tamil Nadu, India, 600036; E-mail: pavanbhukya@smail.iitm.ac.in
[2]Research scientist, Gesellschaft für Anlagen- und Reaktorsicherheit (GRS) gGmbH, Braunschweig, Germany, 38122; E-mail: xuerui.wang@grs.de
[3]Professor, Department of Civil Engineering, Indian Institute of Technology Madras, Chennai, Tamil Nadu, India, 600036; E-mail: arnepalli@iitm.ac.in

ABSTRACT

Microbially driven soil stabilization process known as microbially induced calcite precipitation (MICP) improves the strength and hydraulic characteristics sustainably. However, the biocementation employing MICP treatment depends on numerous factors affecting the biochemical species' migration dynamics (i.e., bacterial and chemical injection source location, number of chemical injection cycles, biochemical injection, and retention durations). The sequence, duration, and location of injections of biochemical species decide the biocement spatial distribution in the soil domain. Therefore, the present study attempts to understand the impact of these influencing factors on the biocement distribution in a heterogeneous soil domain. Accordingly, the study developed a coupled bio-chemo-hydraulic (BCH) model in an open-source code (*OpenGeoSys*) to investigate the influence of diverse injection strategies on biochemical species plume migration and subsequent alterations in the hydraulic characteristics. The results indicated that distinct injection sources for bacteria and chemicals promote closer precipitation to the injection source. However, a single point source for biochemicals migrates the biochemicals front to farther locations, thereby biocement. Besides, multiple chemical injection cycles effectively enhanced precipitation rates compared to single injection cycles. Further, the chemical retention time was crucial in improving the biocement content for both injection scenarios. The chemical injections with retention were comparatively efficient in precipitating higher biocement content than those without retention. Based on the findings from the numerical modeling, the present work also indicated a few guidelines for choosing injection strategies to achieve near-field and far-field precipitation. Besides, the study specified the prominent mechanisms of biochemical species migration under variable injection strategies.

INTRODUCTION

Many geotechnical engineering structures (i.e., slopes, earthen dams, natural deposits for bearing multistorey buildings) need stabilization to meet the design requirements for retaining their engineering properties (shear strength and permeability). Although conventional ground improvement methods such as compaction or lime stabilization are popular, they lack sustainability in the treatment approach. Recently, the microbially induced calcite precipitation

(MICP) process has gained interest due to its ability to enhance engineering behavior with its sustainable treatment method (Fu et al., 2023). The MICP process precipitates biocement (i.e., $CaCO_3$) utilizing bacteria and chemicals (i.e., urea and $CaCl_2$) through an enzymatic reaction. The precipitates fill the voids in the soil mass, increasing the strength and reducing the permeability (Chen et al., 2023; Bhukya et al., 2024a,b). Such ability to alter crucial geotechnical properties of soil has made biocementation applicable to numerous geotechnical and geoenvironmental engineering applications (i.e., slope stabilization, ground improvement, seepage control, surface water containment, erosion control).

Although various laboratory-scale experiments were performed, the larger-scale MICP application is still scarce (Martinez et al., 2013; Montoya and Dejong, 2015). The field-scale applications of MICP are minimal due to the complexity of the processes controlling the reaction (Bhukya et al., 2024b). The biocementation method involves the interactions between the domains of biology (B), chemistry (C), hydraulics (H), and mechanics (M). These BCHM physics control the amount and distribution of precipitated calcium carbonate and subsequent changes the strength and hydraulic properties. In recent times, coupled numerical models have gained interest in simulating the complex phenomena that originated during the MICP treatment through coupled interactions among the domain of B↔C↔H↔M (Wang et al., 2024; Bhukya et al., 2024a,b; Mehrabi and Atefi-Monfared, 2022; Bosch et al., 2024; Li et al., 2024). Application of such coupled models can reduce the uncertainties of the treatment process to some extent. Therefore, numerical models must be utilized as tools to predict the precipitation amount.

Usually, in the MICP treatment, the sequence of injections involves the injection of bacteria first; subsequently, the chemicals are injected. In between, the time is given for the bacteria to attach and chemicals to react, which are known as retention phases. This poses challenges in optimizing the process, as the treatment process variables are higher (Bhukya et al., 2024b). Some of the critical variables fattening MICP treatment efficacy are bacterial and chemical injection source location, number of chemical injection cycles, biochemical injection, and retention durations. In addition, the problem becomes even more challenging with the heterogeneity in the untreated soil, where the key hydraulic property, such as permeability, is supposed to alter due to historical geological processes (Wang et al., 2024).

Considering these challenges, the present study mathematically framed a coupled bio-chemo-hydraulic (BCH) model to understand the influence of injection type, injection and retention duration, and number of chemical injection cycles. In order to study this, a series of cases were considered with two types of injections (i.e., two-point and single-point), with and without chemical retention and varying the chemical injection cycles. Besides, heterogeneity in the domain is another important variable considered for the MICP treatment. Accordingly, the permeability was distributed in log-normal function throughout the two-dimensional domain. A coupled BCH model was developed for the reactive transport simulations using the finite element method in an open-source code, *OpenGeoSys*, *OGS* (Bilke et al., 2019). The influence of mechanical loads on the MICP treatment was disregarded for simplification while optimizing the injections. Overall, the study ascertained the influence of injection type, injection duration, and number of chemical injections on hydraulic characteristics such as porosity and permeability were ascertained.

NUMERICAL MODEL DEVELOPMENT

A coupled BCH model was developed adopting the relevant governing equations and constitutive relations from Wang et al. (2024), as the current study is an extension of our previous work. Hence, the verification and validation of the developed BCH model is not detailed here and can be found in Wang et al. (2024).

The components inside the fluid during the reaction phase of the biocementation process are bacteria, urea, ammonium ions, and calcium. However, due to the lag time between injections (i.e., retentions), the attached bacteria and calcium carbonate accumulate onto the soil's solid surface, considered as attached components. The attached bacteria majorly contribute to the biochemical reaction to happen. Therefore, the attachment of the suspended bacteria onto the solid grains is an essential mechanism that governs the MICP treatment. Moreover, the reaction of biochemicals is initiated after the injection of chemicals, followed by biomass attachment. The significant phenomena that govern the MICP treatment are advection, diffusion, dispersion, biochemical reaction, bacterial attachment, and encapsulation (Bhukya and Arnepalli, 2024). The advection of injected biochemical species majorly contributes to the transport within the soil. Diffusion is a prolonged process that occurs due to a concentration gradient at the molecular level. At the same time, biochemical transport is dependent on dispersion, which is a function of the tortuous flow paths in the soil pores and fluid flow velocity. Usually, the diffusion and dispersion are combined to represent the diffusive-dispersive tensor in the transport equation. Although advection is the dominant transport mechanism, the reaction of biochemicals is a major contributor to the formation of biocement and altering the concentration of chemicals (Fauriel and Laloui, 2012). Besides, the precipitation of calcium carbonate in soil pores reduces the porosity and permeability of the domain (Bhukya et al., 2024b). Alternation in permeability is a crucial factor in changing the advective flow velocity, thereby minimizing the transport rate of chemical species and ultimately affecting the biocement content (Martinez et al., 2013). Overall, bio-chemo-hydraulic processes control the biocementation treatment's efficacy in the absence of mechanical loads.

In the present study, the soil mass is saturated with the single fluid phase (i.e., water). The soil solid grains are assumed incompressible. The fluid within the pores is considered to be compressible. During injection, the biochemical components (i.e., suspended bacteria, urea, ammonium ions, and calcium) are suspended inside the water (Fauriel and Laloui, 2012). At the same time, the attached bacteria and calcium carbonate are sorbed to the soil's solid surface (Bhukya and Arnepalli, 2024). The biochemical reaction rate is first-order kinetically controlled, following Michealis-Menten kinetics. Likewise, the bacterial attachment, straining, and encapsulation rates are first-order rate constants. However, the sorption of chemical species and the growth of bacteria are assumed to be negligible (Fauriel and Laloui, 2012; Wang et al., 2020, Wang et al., 2022, Wang et al., 2024). All the biochemicals are transported according to advective-diffusive-dispersive-reactive processes inside the soil media. Darcy's law governs advective transport, and Fick's law controls diffusive transport. The alterations in flow paths due to pore filling of precipitated calcium carbonate are specified by the permeability relation of Kozeny-Carman equation (Wang et al., 2024).

Mathematical formulation and solution strategy.

The governing equations for simulating the biocementation process consist of the mass balance of fluid for fluid pressure, the mass balance of suspended components in water for concentration changes, and bio-chemo-hydraulic constitutive relations for obtaining unique solutions. Following is the complete mathematical formulation and solution strategy considered in the present study.

Governing equations. The fluid pressure, p (Pa), in the soil pores with porosity (φ) due to applied pressure gradients is evaluated using the mass balance equation of fluid (Eq. 1). The compressibility of the fluid phase with the fluid density, ρ (kg·m^{-3}) is considered with the compressibility coefficient, β (Pa^{-1}). In addition, in the mass balance of fluid, the mass flux of suspended component (i) with molar mass, m^i (kg·kmol^{-1}), and Darcy's fluid flux, $\boldsymbol{q}^i$ (m·s^{-1}) were considered as a source term, $\prod^i = \varphi \cdot R^i \cdot m^i$, with R^i (kmol·m^{-3}·s^{-1}) as the source or sink term based on the reaction.

$$\varphi\rho\beta\frac{\partial p}{\partial t} = \nabla\cdot\frac{\boldsymbol{K}\rho}{\mu}\left(\nabla p - \rho\boldsymbol{g}\right) + \Pi^i \tag{1}$$

Likewise, the mass balance equations of suspended biochemical species are utilized to determine the concentration changes in the soil mass. For any biochemical component i inside the fluid, the mass balance equation is in the form of Eq. (2).

$$\varphi\frac{\partial C^i}{\partial t} = \nabla\cdot\left(\varphi\boldsymbol{D}^i\cdot\nabla C^i\right) - \boldsymbol{q}^i\cdot\nabla C^i + R^i \qquad (i \in \text{bacl, u, NH}_4^+\text{, Ca}^{2+}) \tag{2}$$

where, C^i is the concentration of biochemical species i with bacl as suspended bacteria, u as urea, NH_4^+ as the ammonium ion, Ca^{2+} as the calcium ion (kmol·m^{-3}), and $\boldsymbol{D}^i$ is the diffusion dispersion tensor of respective biochemical species with its components having units of m^2·s^{-1}.

However, during the retention phase of bacteria, the suspended bacteria tend to attach to the soil particles. While the chemicals are retained, the biochemical reaction initiates calcium carbonate formation on the soil solids. The rate of change in concentration of attached bacteria (C^{bacs}) and calcite (C^{CaCO_3}) can be derived from suspended bacteria and reaction rate, respectively. Additionally, the attached bacterial concentration is considered to change with bacterial straining and bacterial encapsulation processes (Eq. 3, 4).

$$\frac{\mathrm{d}C^{\text{bacs}}}{\mathrm{d}t} = \left(k_{\text{att}} + k_{\text{str}}\right)C^{\text{bacl}} - \frac{\Delta C^{\text{CaCO}_3}}{K^{\text{enc}}}C^{\text{bacs}} \tag{3}$$

$$\frac{\mathrm{d}C^{\text{CaCO}_3}}{\mathrm{d}t} = \varphi k_{\text{rea}} \tag{4}$$

where, k_{att} is the attachment rate of bacteria (s^{-1}), k_{str} is the bacterial straining rate (s^{-1}), K^{enc} is the encapsulation rate of bacteria (kg·m^{-3}·s^{-1}), and k_{rea} is the biochemical reaction rate (kmol·m^{-3}·s^{-1}).

As the precipitation of calcium carbonate progresses, the porosity of the soil is altered simultaneously due to pore-filling effects. The rate of change of porosity can be evaluated using the reaction rate (Eq. 5).

$$\frac{\mathrm{d}\varphi}{\mathrm{d}t} = -\frac{1}{\rho^{\text{CaCO}_3}}m^{\text{CaCO}_3}\varphi k_{\text{rea}} \tag{5}$$

where, ρ^{CaCO_3} is the density of calcium carbonate ($kg \cdot m^{-3}$) and m^{CaCO3} is the molar mass of calcite ($kg \cdot kmol^{-1}$).

Constitutive relations. Supplementary relations are necessary to find solutions for the unknown variables of the system of governing equations (Eqs. 1-4). Therefore, the constitutive relations were acquired for each physics to solve flow and biochemical transport equations. The advective fluid flux ($\boldsymbol{q}^i$) due to pressure gradient ($m \cdot s^{-1}$) is given as per Darcy's law (Eq. 6). Moreover, the advective flux ($\boldsymbol{q}^i$) is related to seepage velocity ($\boldsymbol{v}$) and porosity (i.e., $\boldsymbol{q}^i = \varphi \boldsymbol{v}$).

$$\boldsymbol{q} = \varphi \boldsymbol{v} = -\frac{\boldsymbol{K}}{\mu_1} \cdot \left(\nabla p_1 - \rho_1 \boldsymbol{g} \right) \tag{6}$$

The diffusive dispersive tensor ($\boldsymbol{D}^i$) is evaluated as a function of molecular diffusion of biochemical component i ($\boldsymbol{D}_m$) and dispersion coefficients in longitudinal and transverse directions (α_L and α_T). The dispersion of biochemicals is also hindered by the seepage velocity of the fluid ($\boldsymbol{v}$). The overall diffusive-dispersion tensor is given as the combination of the above-mentioned processes (Eq. 7).

$$\boldsymbol{D}^i = \boldsymbol{D}_m{}^i + \left(\alpha_L - \alpha_T \right) \frac{\boldsymbol{v} \otimes \boldsymbol{v}}{|\boldsymbol{v}|} + \alpha_T |\boldsymbol{v}| \boldsymbol{I} \tag{7}$$

The biochemical reaction rate (k_{rea}) is specified using the Michaelis-Menten kinetics equation (Eq. 8), where the substrate is urea with a concentration (C^u) in $kmol \cdot m^{-3}$, and the enzyme release rate is the function of the concentration of total bacteria ($C^{bacl} + C^{bacs}$) in OD and maximum urease rate constant (u_{sp}) in $kmol \cdot m^{-3} \cdot s^{-1} \cdot OD^{-1}$.

$$k_{rea} = u_{sp} \left(C^{bacl} + C^{bacs} \right) \frac{C^u}{k_m + C^u} \tag{8}$$

The reactive source term R^i is the function of the biochemical reaction rate for suspended chemicals ($= \varphi \cdot n_i \cdot k_{rea}$), whereas it is the function of attachment and straining rates for suspended bacteria ($= - \varphi \cdot (k_{att} + k_{str}) \cdot C_{bacl}$). The n_i is the stochiometric coefficient of chemicals, obtained based on the chemical reaction equation ($n_u = -1$, $n_{Ca^{2+}} = -1$, and $n_{NH_4^+} = 2$).

The biocement precipitation occupies the pore spaces and reduces the porosity of the soil mass as per Eq. 5. As the porosity of the soil reduces, the permeability changes due to pore filling simultaneously. To represent this, the Kozeny-Carman relation was adopted to track the changes in permeability with respect to initial permeability (Eq. 9).

$$\boldsymbol{K}_i = \frac{\varphi_i^3}{\left(1 - \varphi_i\right)^2} \frac{\left(1 - \varphi_0\right)^2}{\varphi_0^3} \boldsymbol{K}_0 \tag{9}$$

where, $\boldsymbol{K}_i$ is the current permeability tensor at the current porosity of φ_i with an isotropic permeability of k_i (m^2). Similarly, $\boldsymbol{K}_0$ is the initial permeability tensor at the initial porosity of φ_0 with an isotropic initial permeability of k_0 (m^2)

Numerical strategy. The study utilizes the finite element method to solve the system of governing equations with the operator splitting (OS) approach in OGS (Bilke et al., 2019; Wang et al., 2020, Wang et al., 2024). The OS method solves the component transport equation without a reaction term in the first step, and then the concentration is fed for the reaction term alone and without advective-diffusion terms. This reaction term is simulated with the PHREEQC simulator, and the OGS simulator solves the flow and transport processes. A staggered solution scheme is utilized to solve for fluid pressure first and then biochemical concentrations iteratively. The converged primary variables are utilized to update the permeability of the soil mass. Later, the simulations continued for the next time step until the final step of the simulation.

LARGE-SCALE MICP APPLICATION

The current section discusses the large-scale MICP injections performed by altering various settings in the biochemical injections. As the injections at the field scale are time-consuming compared to laboratory scale studies, the study considered biomass encapsulation's influence on the attached biomass concentration. Considering the scale of the treatment process, the biochemical injections into the soil media must be adjusted to have a region that intersects with bacteria and chemical species plumes for the reaction to initiate (Wang et al., 2024). Otherwise, the biochemicals could simply be transported in opposite directions from the area of interest and flushed out without even reacting. Accordingly, the study aims to understand the influence of injection location, injection cycles of chemicals, and the presence and absence of the chemical retention phase. In addition, geological heterogeneity is considered in terms of permeability, which is another essential variable that alters the flow paths during injections.

At first, the location of bacterial and chemical injection sources was chosen, creating two-point (TP) and single-point (SP) injection sources. Secondly, the number of chemical injection cycles was altered from 5 to 20 for both TP and SP scenarios with multiple chemical injection cycles (1 cycle: 10 h chemical injection, CI + 20 h chemical retention, CR). Finally, the influence of the chemical retention phase was studied for TP and SP cases adopting the chemical retention phase (100 h chemical injection + 200 h chemical retention) and without chemical retention (300 h chemical injection) while maintaining the total duration of the chemical injection cycle constant (i.e., 300 h).

Geometry and boundary conditions.

The large-scale domain of dimensions 100 m (length) × 50 m (depth) was considered for the finite element simulations. The domain was distributed with heterogeneous permeability of widely used log-normal distribution function (f) by varying the initial permeability (k_0) between 1×10^{-16} m^2 to 1×10^{-12} m^2 as per Eq. 10. The mean value of μ and standard deviation of σ were evaluated utilizing the ranges of permeabilities mentioned. The mean value was assumed to be the minimum permeability adopted. However, the standard deviation was considered one-third of the difference in logs of maximum and minimum permeabilities. The log-normal distribution contour of permeabilities is represented in Figure 1 (Wang et al., 2024).

$$f\left(k \mid \mu,\sigma\right) = \frac{1}{k_0 \sigma \sqrt{2\pi}} \exp\left[-\frac{\left(\ln k_0 - \mu\right)^2}{2\sigma^2}\right] \tag{10}$$

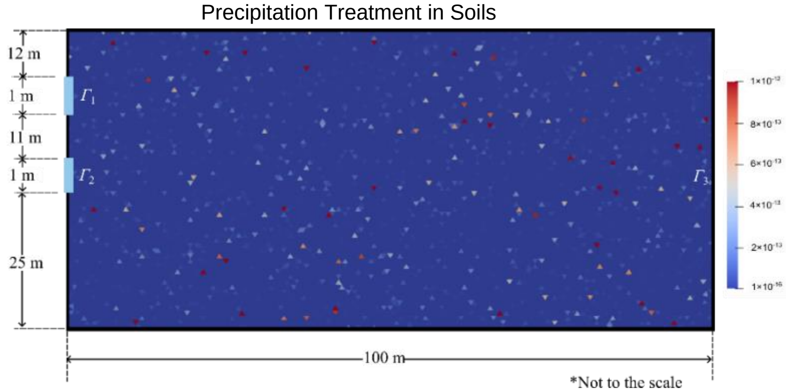

Figure 1. Geometry and boundary conditions of heterogeneously permeable soil domain (100 m × 50 m) for MICP injections

The considered domain is assumed to have an initial fluid pressure (p_0) of 10 MPa and zero biochemical concentrations for all the cases. The boundary conditions on the left boundaries (Γ_1, Γ_2) were based on the injection type. For two-point injection (TP), the bacteria are injected from the surface (Γ_1), and the chemicals are injected from the surface (Γ_2). On the other hand, bacteria and chemicals were injected from the surface (Γ_2) alone during single-point injection (SP). But, during both the injection types (TP and SP), the right boundary (Γ_3) is subjected to constant fluid pressure (p = 10 MPa), no fluid flux ($\boldsymbol{q}\cdot\boldsymbol{n} = 0$), and natural mass flux ($\boldsymbol{D}\varphi\nabla C\cdot\boldsymbol{n} = 0$). The input parameters for the large-scale simulations are available in our previous work (Wang et al., 2024).

RESULTS AND DISCUSSION

The biochemical injections were performed for various scenarios with varying injection types, number of chemical injection cycles, and in the presence and absence of retention phase. The influence of MICP injections for all the cases was reported in terms of permeability ratio (k/k_0) along the line of interest at a mid-depth of 25 m (Figure 2a-d). The permeability ratio indicates the ratio of final permeability (k) after MICP treatment to the initial permeability (k_0), a parameter that indicates the effect of biocementation.

The SP injections precipitated calcite far from the injection source with minimal calcite content (Figure 2a). On the contrary, the two-point injections resulted in closer precipitation to the injection source with a more significant precipitation amount (Figure 2b). It can be observed from the permeability ratio plots that a significant reduction in permeability was observed for TP injections and a lower reduction of permeability for SP injection from the initial state (Figure 2a,b). At the same time, as the number of chemical injection cycles (CI+CR) increased from 5 to 20, the permeability ratio was lowered proportionally, indicating the influence of chemical injection cycles (Figure 2a,b). However, for the SP injections, the permeability ratio profiles are traversed farther as the number of chemical injections increases from 5 to 20. This is due to the fluid displacement effect on bacteria when chemicals are injected from the same injection source, Γ_2 (Figure 2a). Because of the fluid displacement effect, the bacteria were no longer available for reaction near the SP injection source. Thus, after 15 CI cycles through SP injection, the residual bacteria available for reaction at approximately 15 m was consumed completely, thereby limiting the precipitation sites in the case of 20 CI cycles (Figure 2a). In contrast, due to a distinct BI and CI source (Γ_1 and Γ_2) in the case of TP injections, the bacterial profiles were mostly unaltered, resulting in a progressive biocementation and permeability reduction with an increase in CI cycles (Figure 2b).

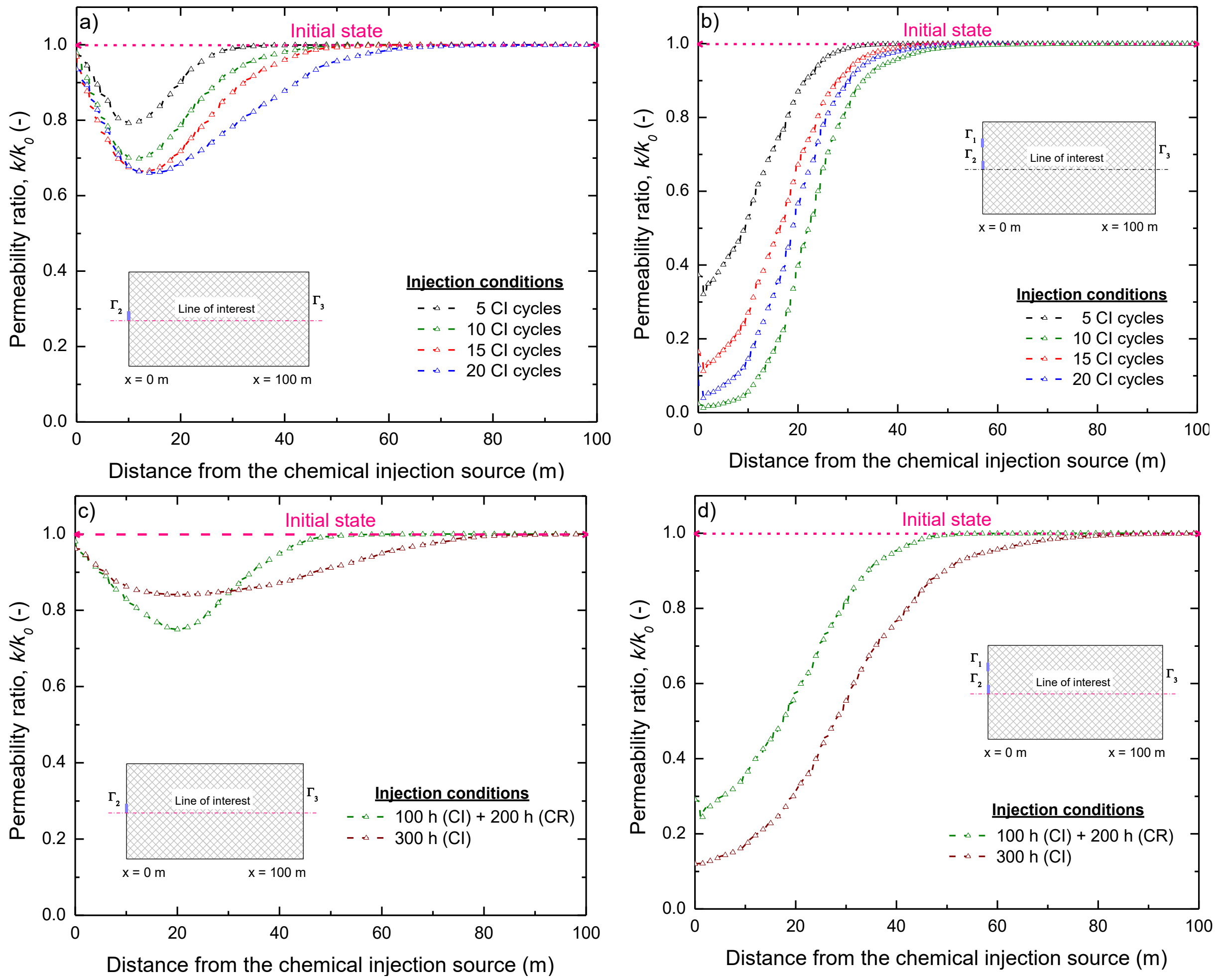

Figure 2. Permeability ratio (k/k_0) a) SP injection with multiple chemical injection cycles b) TP injection with multiple chemical injection cycles c) SP injection with and without chemical retention effects d) TP injection with and without chemical retention effects

For the flexible chemical retention (CR) phase cases, the instances of SP injection with chemical retention have resulted in a more significant reduction in permeability than those with pure chemical injection (Figure 2c). Interestingly, in the case of two-point injection, the cases without retention (i.e., pure chemical injection) have resulted in higher precipitation, thereby lower permeability (Figure 2d). However, similar to the previous observation, the SP injections have resulted in a farther and lower reduction in permeability compared to TP injections (Figure 2c, d).

The two-dimensional porosity contours at the end of MICP treatment revealed further insights into the influence of injection conditions. The TP injection strategy considering multiple and single CI cycles produced near-field mixing of biochemical species due to distinct BI and CI sources, resulting in lower porosity near the injection source (Figure 3a,b). In contrast, SP injection with and without CR revealed that far-field mixing of biochemical species occurred due to the fluid displacement effect as the chemicals were injected from the same injection source (Figure 3c,d). The multiple CI cycles with the TP approach produced a considerable porosity change from an initial porosity (φ_0 = 0.4) compared to a single stretch of chemical injection and retention

(Figure 3a,b). On the other hand, the SP injection with retention has shown a relatively higher porosity change compared to the pure CI scenario (Figure 3c,d). Therefore, a closer permeability reduction was observed using the TP approach (Figure 2b,d), and farther permeability changes were observed for the SP injection strategy (Figure 2a,c).

Overall, to enhance the biocementation levels, an increase in the number of injection cycles and the application of the chemical retention phase is recommended. Although pure chemical injection has resulted in higher precipitation in TP injections, they consume a considerable amount of chemicals, which is uneconomical compared to the application of the retention phase. Therefore, chemical retention is recommended for all injection types. Besides, if higher precipitation is required at near-field distances, TP injection with multiple chemical injections and retentions is recommended. On the contrary, SP injections with multiple chemical injection and retention phases are recommended for far-field precipitation. Nevertheless, further studies are necessary to optimize the far-field injections for specific calcite content, as the dilution effects result in lower calcite than anticipated with the SP injection strategy.

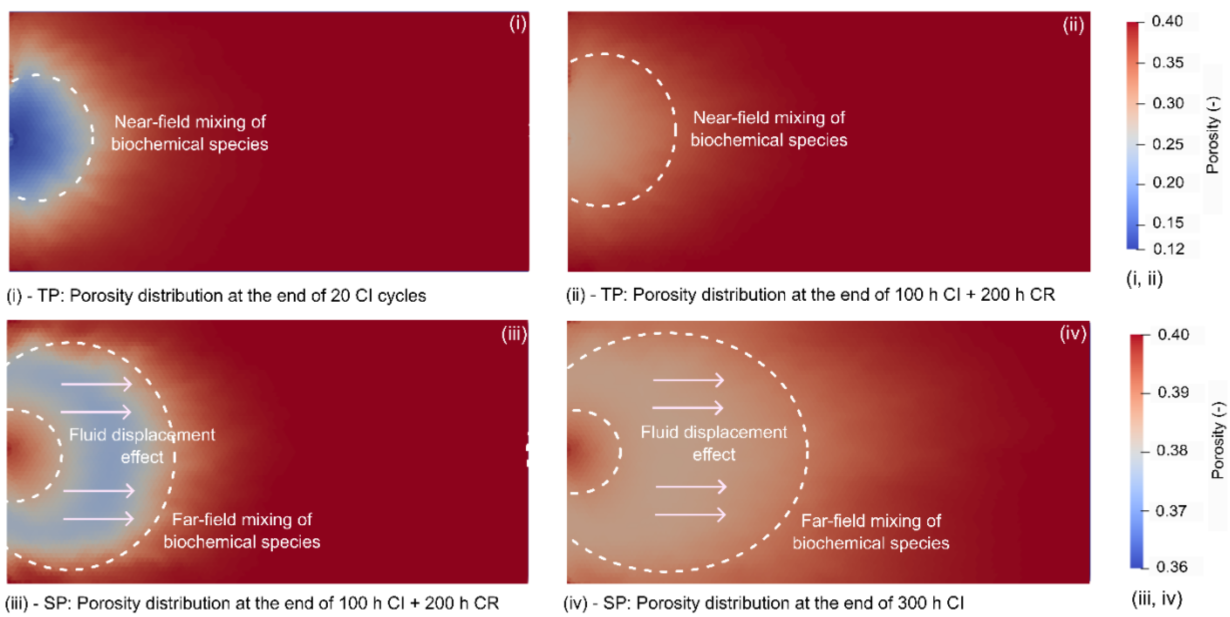

Figure 3. Porosity (φ) distribution under multiple injection scenarios i) TP injection with 20 CI cycles ii) TP injection with 1 CI cycle iii) SP injection with 1 CI injection cycle iii) SP injection with 1 CI cycle without CR

CONCLUSIONS

The present study developed a coupled bio-chemo-hydraulic model to understand the MICP treatment at a larger scale in an open-source code *OpenGeoSys*. An operator-splitting approach was used to solve the governing equations using the finite element method in a staggered manner. The developed model was validated using laboratory-scale experimental observations before employing it for large-scale simulations. Also, a realistic representation of heterogeneity in the domain in terms of permeability was considered in the current work. The present work attempted to understand the influence of injection type, the number of chemical injection cycles, and the presence of the chemical retention phase. The observations from the biochemical injections performed indicated that two-point injection promotes nearer precipitation, and single-point injection distributes the biocement peak far from the injection source. Also, multiple chemical injections and the presence of a chemical retention phase are recommended to enhance the further precipitation in both injection types. The study indicated that the permeability reduction was the most significant for two-point injections with the maximum number of chemical injection cycles. The present work provided probable scenarios that are possible for biochemical injections and provided guidance in choosing a specific injection strategy. However, further studies are recommended to optimize various injection durations that are involved in the treatment process.

ACKNOWLEDGEMENT

The authors gratefully acknowledge the support from the *OpenGeoSys* community. Also, this research was partially funded by the Prime Minister Research Fellowship, Ministry of Education, Government of India with the project number SB21221901CEPMRF008347.

REFERENCES

Bhukya, P.K., Adla, N. and Arnepalli, D.N. (2024a). "Coupled bio-chemo-hydro-mechanical modeling of microbially induced calcite precipitation process considering biomass encapsulation using a micro-scale relationship." *J. Rock Mech. and Geotech. Eng.*, 16(7), 2775-2789.

Bhukya, P. K., Adla, N., and Arnepalli, D. N. (2024b). "Numerical Optimisation of Microbially Induced Calcite Precipitation (MICP) Injection Strategies for Sealing the Aquifer's Leakage Paths for CO_2 Geosequestration Application." *Adv. Water Resour.*, 104800.

Bhukya, P. K., and Arnepalli, D. N. (2024). "Coupled modelling framework for evaluating the influence of bacterial attachment models on the bio-chemo-hydro-mechanical behaviour during microbially induced calcite precipitation treatment in soils." *Comp. Geotech.*, *173*, 106561.

Bilke, L., Flemisch, B., Kalbacher, T., Kolditz, O., Helmig, R. and Nagel, T. (2019). "Development of open-source porous media simulators: principles and experiences." *Trans. Porous Med.*, 130, 337-361.

Bosch, J.A., Terzis, D. and Laloui, L. (2024). "A bio-chemo-hydro-mechanical model of transport, strength and deformation for bio-cementation applications." *Acta Geotech.*, 19(5), 2805-2821.

Chen, Y., Han, Y., Zhang, X., Sarajpoor, S., Zhang, S. and Yao, X. (2023). "Experimental study on permeability and strength characteristics of MICP-treated calcareous sand." *Biogeotechnics*, 1(3), 100034.

Fu, T., Saracho, AC and Haigh, S.K. (2023). "Microbially induced carbonate precipitation (MICP) for soil strengthening: A comprehensive review." *Biogeotechnics*, 1(1), 100002.

Fauriel, S., and Laloui, L. (2012). "A bio-chemo-hydro-mechanical model for microbially induced calcite precipitation in soils." *Comp. Geotech.*, 46, 104-120.

Martinez, B.C., DeJong, J.T., Ginn, T.R., Montoya, B.M., Barkouki, T.H., Hunt, C., Tanyu, B. and Major, D. (2013). "Experimental optimization of microbial-induced carbonate precipitation for soil improvement." *J. Geotech. Geoenviron. Eng.*, 139(4), 587-598.

Montoya, B.M. and DeJong, J.T. (2015). "Stress-strain behavior of sands cemented by microbially induced calcite precipitation." *J. Geotech. Geoenviron. Eng.*, 141(6), 04015019.

Mehrabi, R. and Atefi-Monfared, K. (2022). “A coupled bio-chemo-hydro-mechanical model for bio-cementation in porous media.” *Can. Geotech. J.*, 59(7), 1266-1280.

Wang, X. and Nackenhorst, U. (2020). “A coupled bio-chemo-hydraulic model to predict porosity and permeability reduction during microbially induced calcite precipitation.” *Adv. Water Resour.*, 140, 103563.

Wang, X. and Nackenhorst, U. (2022). “Micro-feature-motivated numerical analysis of the coupled bio-chemo-hydro-mechanical behaviour in MICP.” *Acta Geotech.*, 17(10), 4537-4553.

Wang, X., Bhukya, P. K., Arnepalli, D. N., and Chen, S. (2024). “Coupled multiphysical model for investigation of influence factors in the application of microbially induced calcite precipitation.” *J. Rock Mech. Geotech. Eng.*, 16(6), 2232-2249.

Li, Y., Guo, Z., Wang, L., Sun, X. and Zhu, Y. (2024). “Numerical analysis of Microbially induced calcite precipitation and Enzyme induced calcite precipitation in Calcareous Sand: Multi-process and Biochemical reactions.” *J. Rock Mech. Geotech. Eng.* (In press)